Modeling of Lung's Electrical Impedance using Fractional Calculus for Analysis of heat generation during RF-Ablation

Nozomu Yamazaki, *IEEE Member*, Yo Kobayashi, *IEEE Member*, Hayato Kikuchi, Yosuke Isobe, XiaoWei Lu, *IEEE Member*, Tomoyuki Miyashita, *IEEE Member*, Masakatsu G. Fujie, *IEEE Fellow*

***Abstract*— Recently, Radio Frequency Ablation (RFA) is becoming a popular therapy for various cancers such as liver, breast, or lung cancer. RFA is one kinds of thermal therapy. However, it has been often reported about excessive ablation or non-ablation due to difficult control of ablation energy. In order to solve these difficulties, we have been proposed robotized RF-ablation system for precise cancer treatment. We have been tried to control heat energy by control of electromagnetic-wave frequency.**

In this paper, we reported about relation among electrical impedance of lung, lung's internal air volumes, and heat energy by use of electromagnetic-wave. In case of RFA for lung cancer, heat energy depends on electrical impedance and lung's internal air volumes. Electrical impedance has the dependence of electromagnetic-wave frequency and the dependence of lung's internal air volumes. Therefore, firstly we considered about fractional calculus model between lung's internal air volumes and electrical impedance. Secondly, we measured electric impedance frequency characteristic of lung with change of lung's internal air volumes. The measured and modeled results showed that use of fractional calculus realized high accurate model for electrical impedance of lung. And, from the results of numerical analysis of heat energy, it is supposed that control of electromagnetic-wave frequency has a small effectiveness for lung tissue ablation even if lung includes abundant air.

I. Introduction

A. Radio frequency ablation (RFA) for cancer

Radio frequency ablation (RFA) is an important method for treating cancers and has increasingly been used over the past few years [1] ~ [3]. RFA involves an electrode-needle. This needle percutaneously inserted into a cancer and input RF energy for cancer, whereupon the temperature of the tissue rises due to the ionic agitation generated by the electromagnetic-wave at 470 kHz. Tissue coagulation occurs due to a result of protein denaturation when a temperature of tissue around RF-electrode reaches at about 60°C. Subsequently, moisture evaporation occurs and a cancer becomes completely necrotic at 70-80°C. Therefore, the RFA is able to provide a minimally invasive treatment and shorter hospital stay for patients. The effectiveness of RFA for cancers is higher curable almost the same as traditional open surgery. RFA is chose and operated widely. An ablation mechanism of RFA is shown in Figure 1. When it turns on radio-wave to a cancer, it generates on electrical field around RF-electrode and Joule's heat is generated by ionic agitation of. If it progress an ablation, an electrical impedance value will be higher due to coagulation of tissue around RF-electrode. If an electrical impedance value reaches 1000[Ω], radio-wave generator stop automatically. This is so called "Roll-off". Therefore, Radio-wave generator judges ablation progress from an electrical impedance value.

B. RFA for lung cancer

Recently, the effectiveness of RFA has been reported for liver cancer and breast cancer, and as a consequence RFA is now beginning to be applied in lung cancer. The RFA procedure for lung cancer is to percutaneously puncture the cancer with the RF electrode. Subsequently using X-ray CT, the operator checks an ablation region and the relative positions of the cancer and RF electrode. Finally, the radio wave is generated for cancer.

A characteristic of RFA for lung cancer is that a lung contains abundant air during surgical operation. From the view point of material properties, thermal conductivity of air is very low. Therefore, it is generally said that a lung's internal air focuses the RF energy from an electrode needle onto a limited region. Thus, it has possibility that a lung is more suitable than the breast, liver or bone for ablation [2].

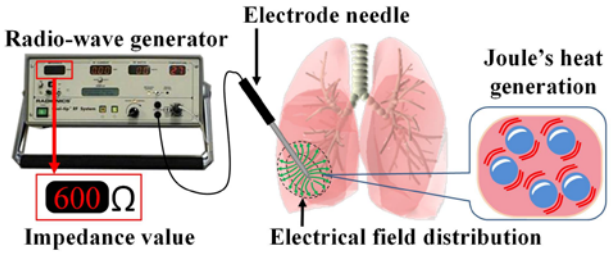

(a) Mechanism of heat generation

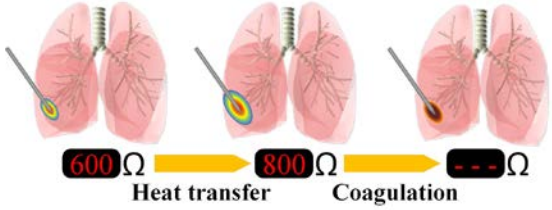

(b) Tissue coagulation process with impedance value

Fig. 1 Ablation process under using radio-wave

Manuscript received April 7, 2014. This work was supported in part by JSPS "Strategic Young Researcher Overseas Visits Program for Accelerating Brain Circulation", JSPS KAKENHI 25·5622 and and MEXT "Takuetsu Program".

N. Yamazaki, members of the Graduate Schools of Advanced Science and Engineering, Waseda University, Japan. (59-309, 3-4-1, Okubo, Shinjuku Ward, Tokyo, Japan, e-mail: nozomu0626@akane.waseda.jp, tel: +81-3-5286-3412, fax: +81-3-5291-8269)

Y. Kobayashi, member of the Research Institute for Science and Engineering, Waseda University, Japan.

H. Kikuchi, Y. Isobe, X. Lu, member of the Graduate Schools of Creative Science and Engineering, Waseda University, Japan.

Y. Kobayashi, T. Miyashita, M. G. Fujie, Members of the Faculty of the Graduate School of Science and Engineering, Waseda University, Japan.

C. RFA for lung cancer

However, RFA has difficulties instead of above mentioned merits. It has been often reported about excessive-ablation or non-ablation for a cancer. Because ablation energy emitted from RF-electrode is difficult to control with tissue coagulation progress. In case of RFA for a lung cancer, it is often occurred non-ablation due to changing lung's internal air volume [4] ~ [5]. Internal air of lung has influence of heat energy from RF-electrode. An air-volume always changes by respiration or collapse. Thus, RFA for lung cancer is not able to generate constant heat energy. From our study, electrical conductivity of lung is decreasing with increasing lung's internal air volumes. Electrical conductivity is related to heat energy from RF-electrode. If electrical conductivity is decrease, heat energy is decrease. Therefore, in order to do precise ablation for lung cancer, it has to consider about an influence of lung's internal air to ablation.

II. OBJECTIVES

In order to realize precise cancer ablation at radio-wave band, we have been proposed robotized RF-ablation system [6]. We have been tried to control heat energy for cancer by control of electromagnetic-wave frequency [7]. The system optimizes RF energy for a lung cancer with each various internal air volumes of lung.

The objective of this study is modeling of lung's electrical impedance using fractional calculus for analysis of heat generation during RF-Ablation. Fractional calculus numerical model is able to represent electrical characteristic of organ high accurately. If it develops an electrical impedance model, it is able to analyze a generation of heat energy from RF-electrode. C. L. Brace has been already mentioned about relationship between electromagnetic-wave frequency and heat energy generation [2]. However, it has not been mentioned about precise electrical impedance model of organ and analysis methods. Therefore, the novelty work of this study is clearer the relationship among with electrical impedance, electromagnetic frequency, and heat generation and each lung's internal air volumes.

III. MATERIAL AND METHOD

To analyze the relationship among with electrical impedance, frequency of electromagnetic-wave, and internal air volumes of lung, firstly we measured electrical impedance of lung with changing lung's internal air volume. Secondly, we modeled and analyzed measurement values by use of equivalent circuit model with fractional calculus. Finally, we numerically analyzed about the relationship between electrical impedance and heat generation each lung internal air volume.

A. Modeling of lung's electric impedance frequency characteristic

We modeled electric impedance frequency characteristic of lung by using Constant Phase Element (CPE) equivalent circuit model [8] ~ [9]. An image of CPE equivalent circuit model is shown in Figure 2. CPE has the feature that the circuit element has not only direct resistance element but also capacitance element. The feature of two circuit element is able to be represented one circuit element by use of fractional calculus numerical model. Therefore CPE have drawn as image of Figure 2. Usually, tissue cell is composed outer cell liquid, inner cell liquid, and cell membrane like as Figure 3(a). Where, Outer cell and inner cell resistance are bigger influence than their capacitance. On the other hand, cell membrane capacitance is bigger influence than this resistance. Thus, Figure 3(a) is introduced to a simple equivalent circuit model like as Figure 3(b). It seems that Figure 2 and Figure 3(b) is very similar circuit model. In actual case, it is difficult to separate direct resistance element and capacitance element. Therefore, we used CPE for modeling electrical impedance.

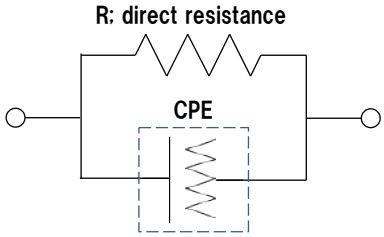

Fig. 2 Simple image of fractional equivalent circuit model of bio-tissue

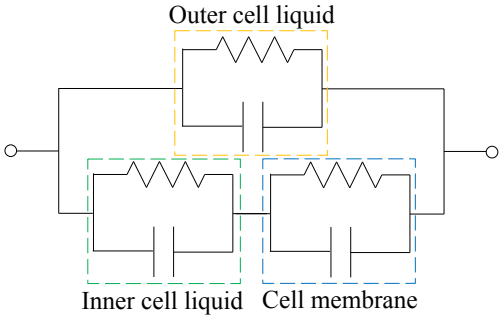

(a) Equivalent circuit model of each cell part

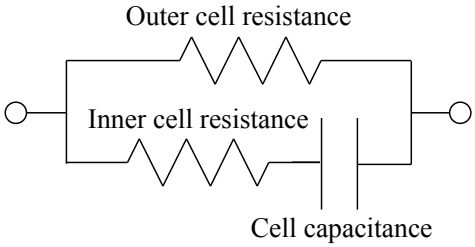

(b) Most simple equivalent circuit model of tissue cell

Fig. 3 Equivalent circuit model of tissue cell

Before modeling of electric impedance frequency characteristic of lung, we mention about the numerical model of CPE with equations (1) ~ (6).

$$Z_{CPE} = \frac{1}{(j\omega RC)^p} \tag{1}$$

$$Z_{CPE} = Z' - jZ'' \tag{2}$$

$$Z' = \frac{1}{\omega^p R^{p-1} C^p} \cos\left(\frac{\pi}{2} p\right) \tag{3}$$

$$Z'' = \frac{1}{\omega^p R^{p-1} C^p} \sin\left(\frac{\pi}{2} p\right) \tag{4}$$

$$|Z_{CPE}| = \frac{1}{\omega^p R^{p-1} C^p} \tag{5}$$

$$\theta = 90 \times p \tag{6}$$

Where, Z_{CPE} is complex impedance [Ω], Z' is real part of impedance element [Ω], Z'' is imaginary part of impedance element [Ω], ω is angular frequency of electromagnetic-wave [rad/s], R is direct resistance [Ω], C is capacitance [F], p is CPE index which depends on target sample and the value range is $0 < p < 1$, $|Z_{CPE}|$ is arbitrary value of electric impedance [Ω], and θ is phase difference [degree] which is between input voltage and output voltage.

From eq. (3) and (4), if CPE index takes a value at 0, Z'' takes a value at 0. Thus, $p = 0$ means that $|Z_{CPE}|$ includes only direct resistance element and real component of impedance element. While on the other hand, in a case at $p = 1$, $|Z_{CPE}|$ includes only capacitance element and imaginary component of impedance element. Therefore, CPE index decides on a ratio of impedance value of real part and imaginary part. The ratio doesn't depend on angular frequency. The phase difference depends on CPE index and a value of phase difference doesn't change with changing angular frequency. It means if once it decides on a value of CPE index, it decides on a value of phase difference. A value of phase difference doesn't change all frequency domains. Therefore, equivalent circuit model of CPE is so called "constant phase element".

However, in case of actual measurement, it is supposed that the phase difference changes with changing angular frequency. Therefore, it needs consider about change of phase deference which occurs due to influence of direct resistance element like as Figure 2. The numerical model of Figure 2 is introduced to equations (7) ~ (12).

$$Z_{CCP} = \frac{R}{R + (j\omega RC)^p} \tag{7}$$

Where, eq. (7) is represented to eq. (8) from eq. (9)

$$Z_{CCP} = \frac{R}{R + R^p C^p (\cos\theta + j \sin\theta)} \tag{8}$$

$$(j\omega)^p = \cos\theta + j \sin\theta \tag{9}$$

Eq. (10) is introduced by rationalization of eq. (8).

$$Z_{CCP} = \frac{R(R + (RC)^p \cos\theta)}{R^2 + (RC)^p \cos\theta + (RC)^{2p}} - j \frac{R \cdot (RC)^p \sin\theta}{R^2 + (RC)^p \cos\theta + (RC)^{2p}} \tag{10}$$

In comparison with eq. (2) and eq. (10), our proposal model's Z' and Z'' represented below eq. (11) and (12).

$$Z'_{CCP} = \frac{R(R + (RC)^p \cos\theta)}{R^2 + 2(RC)^p \cos\theta + (RC)^{2p}} \tag{11}$$

$$Z''_{CCP} = \frac{R \cdot (RC)^p \sin\theta}{R^2 + 2(RC)^p \cos\theta + (RC)^{2p}} \tag{12}$$

Thus, $|Z_{CCP}|$ is calculated to eq. (13) from eq. (11) and (12).

$$|Z_{CCP}| = \frac{R}{\sqrt{R^2 + 2(RC)^p \cos\theta + (RC)^{2p}}} \tag{13}$$

By use of $|Z_{CCP}|$ and θ, eq. (11) and eq. (12) are represented eq. (14) and eq. (15) again.

$$Z'_{CCP} = |Z_{CCP}| \cos\theta \tag{14}$$

$$Z''_{CCP} = |Z_{CCP}| \sin\theta \tag{15}$$

Where, a most difference between CPE only model and our proposal model is that phase difference change with changing frequency. Therefore, our proposal model needs that CPE index is depending on angular frequency. CPE index $p(\omega)$ is introduced to eq. (16) under a frequency range between 10[kHz] to 1000[kHz]. We decided on coefficient α, β, direct resistance R based on result of actual measurement. These values were related as lung's internal pressure. It's exactly mentioned about chapter IV.

$$p = \frac{\alpha \log_{10} \omega + \beta}{90} \tag{16}$$

Due to a change of CPE index with changing angular frequency, a ratio of Z'_{CCP} and Z''_{CCP} change with increasing frequency. The relationship between Z'_{CCP} and Z''_{CCP} is drawing a semicircle. Where, numerical model of the relationship represents eq. (17).

$$\left(Z'_{CCP} - \frac{R(R + (RC)^p \cos\theta)}{R^2 + 2(RC)^p \cos\theta + (RC)^{2p}}\right)^2 + (Z''_{CCP})^2 = \left(\frac{(RC)^p}{1 + 2(RC)^p \cos\theta + (RC)^{2p}}\right)^2 \tag{17}$$

The meanings of eq. (17) is that the relationship between Z'_{CCP} and Z''_{CCP} is drawing a suppression semicircle with a center point (a[Ω], b[Ω]) and radius r[Ω]. Generally, this semicircle and drawing plots are so called "Cole-Cole Plot" which represents result of fractional calculus [8] ~ [9]. We had applied and modeled to "Cole-Cole Plot" for electric impedance frequency characteristic of lung with change of lung's internal pressure. eq. (18) and eq. (19) are representing coordinate center and radius of "Cole-Cole Plot".

$$(a, b) = \left(\frac{R^2}{R^2 + 2(RC)^p \cos\theta + (RC)^{2p}}, 0\right) \tag{18}$$

$$r = \frac{R(RC)^p}{\sqrt{R^2 + 2(RC)^p \cos\theta + (RC)^{2p}}} \tag{19}$$

B. *Measurement of electrical impedance of lung*

We measured electrical impedance of lung with change of internal air volume under *in vitro* experiment where used three individual of swine pig lungs. The measurement situation is shown in Figure 4. In order to measure material properties of lung, we have developed lung's internal air pressure control unit [5]. The unit consists from air compressor, solenoid valves, and a pressure sensor. First of all, it set target pressure of lung and air compressor send air to a lung. When lung's internal pressure reaches target value, solenoid valve change an air flow port. Thus, the unit is able to control lung's internal air volumes and steady keep size of lung. After the unit kept size of lung, we measured electrical impedance by use of impedance analyzer which is commercialized by HIOKI E.E. CORPORATION (CHEMICAL IMPEDANCE METER 3532-80®). This impedance analyzer measure electrical impedance value by "Four Electrodes Method with Alternating current". The simple image of measurement principle is shown in Figure 5 and array of measurement electrodes is shown in Figure 6.

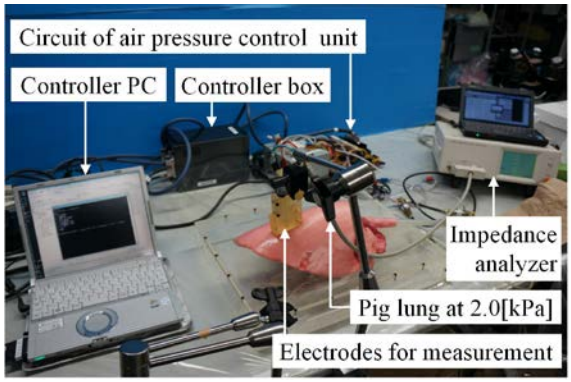

Fig. 4 Measurement situation of electrical impedance

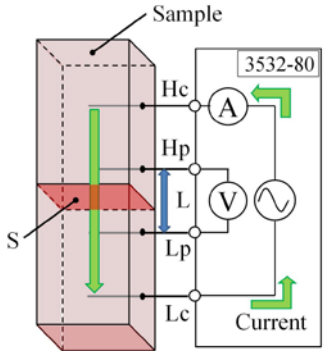

Fig. 5 Four Electrodes Method with Alternating current

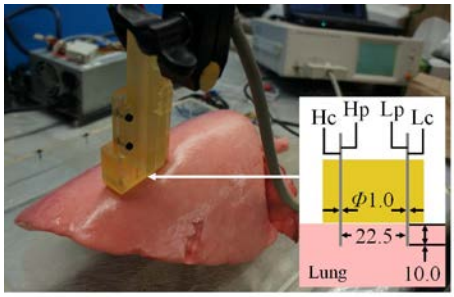

Fig. 6 Array of electrodes

The measurement principle of Four Electrodes Method with Alternating current is that firstly four electrodes insert to a sample. Secondly, it generates electromagnetic-wave with alternating current from Hc terminal to Lc. And, it measure a voltage through the sample between Hp terminal and Lp terminal. Finally it detected on a current through a sample.

In case of lung, we use two electrodes and these inserted into lung and the depth of inserted electrode was 10[mm] from lung surface. The distance between two electrodes is 22.5[mm]. One electrode connects to Hc and Hp and the other electrode connects to Lc and Lp. The first reason why we measured electrical impedance by not four electrodes but two electrodes is to measure voltage and current at same point. And, the second reason is to suppress an influence of flow out of lung's internal air at electrode insertion ports. Under this experimental condition, we measured electrical characteristic of lung with change of lung's internal pressure at 0[kPa], 0.2[kPa], 0.5[kPa], 1.0[kPa] and 2.0[kPa]. Where 0[kPa] means that a lung doesn't contain air and at 2.0[kPa] means that a lung is aerated to maximum size. The measurement frequency range of electromagnetic-wave frequency is between 4[Hz] to 1000[kHz]. This range include the frequency of RFA at 470[kHz] and it is able to analyze a behavior of electrical impedance with a central focus on 470[kHz]. The results are shown in Figure 7 and Figure 8.

Figure 7 shows the bode diagram of one individual in frequency domain. Impedance frequency characteristic of all trials were almost the same behavior. Therefore, we choice and shows one individual result. From Figure 7, absolute value of electric impedance $|Z|$ [Ω] was decreasing with increasing frequency of electromagnetic-wave at each internal pressure. Phase deference between input voltage and output current was decreasing until about 10[kHz] and increasing from 10[kHz] to 1000[kHz] at each internal pressure. It was occurred two different behaviors of electrical characteristic at each pressure. When internal pressure of lung was increased, the value of electrical impedance was decrease. And, when internal pressure of lung was increased, the value of phase difference at each pressure was decreased until about 10[kHz] and the phase difference values was converged almost the same value with increasing frequency from 10[kHz] to 1000[kHz].

Figure 8 shows impedance values of real part and imaginary part. Real part Z' [Ω] means direct resistance element of electrical impedance. And, imaginary part Z''[Ω] means capacitance element of electrical impedance. From Figure 8, Z' was decreasing with increasing frequency of electromagnetic-wave. The difference between Z' and Z''[Ω] was that Z'' was increasing with increasing frequency of electromagnetic-wave from around 10[kHz] until 1000[kHz]. The behaviors of electrical impedance values in real part and imaginary part were almost the same in each pressure of lung.

From experimental result, it is supposed that lung's internal air has more influence on absolute value of electric impedance $|Z|$ than phase difference.

We tried modeling of lung's electrical impedance by use of these experimental results.

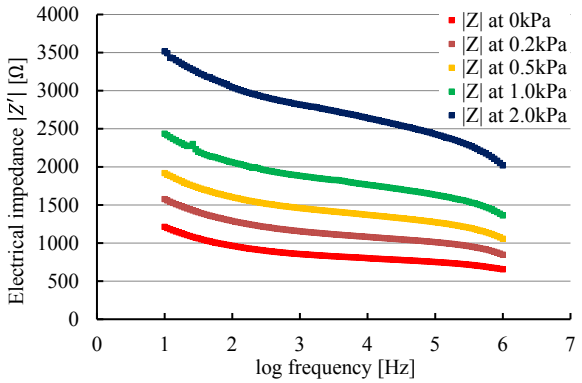

(a) Electrical impedance vs log frequency

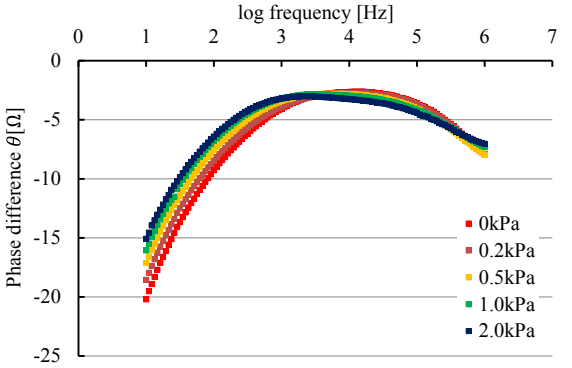

(b) Phase deference vs log frequency

Fig. 7 Bode diagram of individual 1 at each pressure

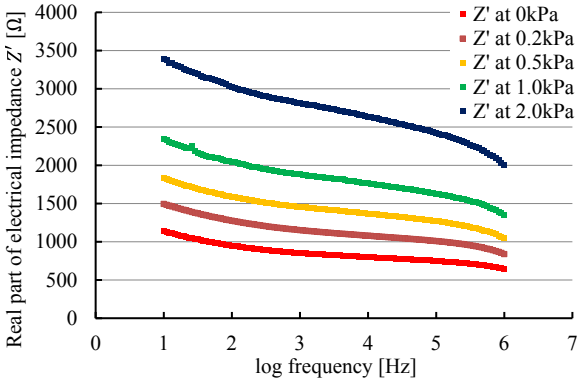

(a) variation of real part value

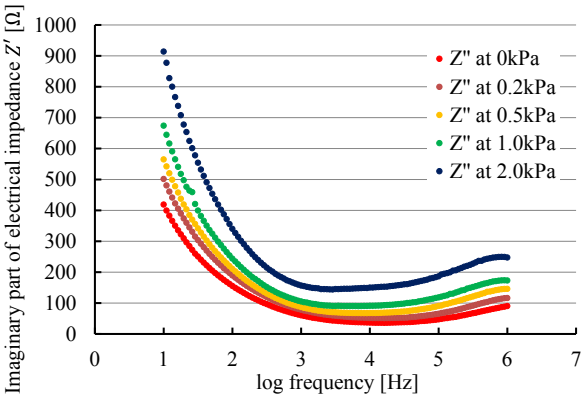

(b) variation of imaginary part value

Fig. 8 Electrical impedance value of individual 1 at each pressure

IV. Result

Figure 9 shows the result of modeling for electric impedance frequency characteristic of lung with change of lung's internal pressure. The frequency range was between 10[kHz] to 1000[kHz]. It seems that our proposal model was very matching the experimental measured values under three individuals. Therefore, we show the result of individual 1 for easy to understand the behavior of modeling values. Table 1 shows use of each parameter for Z'_{CCP} and Z''_{CCP} modeling. From table 1, direct resistance element values at each pressure were very different in each individual.

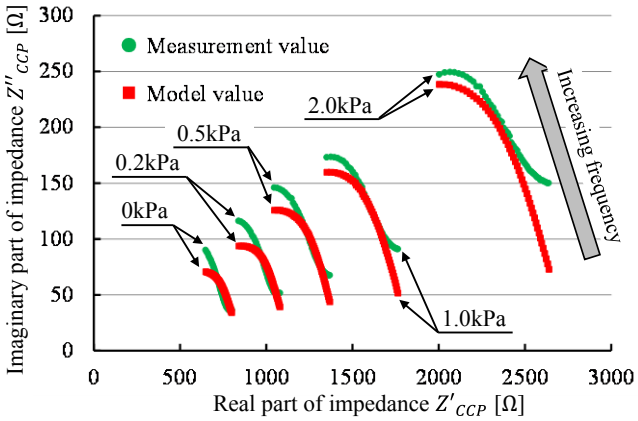

Fig. 9 Cole-Cole Plot of individual 1

Table 1 Each parameter for modeling electrical impedance

Individual 1					
Pressure [kPa]	0	0.2	0.5	1.0	2.0
α	-2.02	-2.27	-2.63	-2.59	-2.62
β	6.98	8.62	10.6	10.7	11.0
R [kΩ]	8	12	20	50	200
Individual 2					
Pressure [kPa]	0	0.2	0.5	1.0	2.0
α	-4.44	-4.43	-4.07	-3.91	-2.65
β	17.5	16.6	15.3	14.0	7.27
R [kΩ]	30	40	50	100	200
Individual 3					
Pressure [kPa]	0	0.2	0.5	1.0	2.0
α	-3.02	-1.98	-1.61	-1.64	-1.14
β	12.5	7.41	5.28	5.64	2.66
R [kΩ]	10	30	40	50	100

Table 2 Accuracy of modeling value comparison with measurement value

Individual 1					
Pressure [kPa]	0	0.2	0.5	1.0	2.0
Maximum error of Z' %	0.376	0.336	0.252	0.124	0.124
Minimum error of Z' %	0.002	0.024	0.001	0.001	0.026
Maximum error of Z'' %	23.29	24.44	35.32	43.53	51.44
Minimum error of Z'' %	0.745	0.377	0.169	0.110	3.480
Individual 2					
Pressure [kPa]	0	0.2	0.5	1.0	2.0
Maximum error of Z' %	0.495	0.398	0.342	0.194	0.111
Minimum error of Z' %	0.001	0.002	0.031	0.001	0.003
Maximum error of Z'' %	24.89	21.28	18.86	13.45	7.15
Minimum error of Z'' %	0.005	0.014	0.179	0.010	0.927
Individual 3					
Pressure [kPa]	0	0.2	0.5	1.0	2.0
Maximum error of Z' %	0.400	0.136	0.094	0.072	0.047
Minimum error of Z' %	0.001	0.002	0.001	0.001	0.001
Maximum error of Z'' %	44.17	29.49	25.58	20.05	10.40
Minimum error of Z'' %	0.046	0.410	0.184	0.184	0.005

V. DISCUSSION

A) Accuracy of proposal model

From table 2, our proposal model had a large error in Z''_{CCP}. The maximum error is about 51.44% at 2.0[kPa] of individual 1. However, Z''_{CCP} is very small value in comparison with Z'_{CCP}. The value of heat energy generation depends on Z'_{CCP} and modeling of Z'_{CCP} was very match comparison with measured values. Therefore, our proposal model is able to analyze energy of heat generation even if it has the above error of Z''_{CCP}.

The reason why our model was match the electric impedance frequency characteristic of lung, our model consider about non-linearity of organ's electrical properties by use of fractional calculus model.

B) The relationship between heat energy generation and frequency of electromagnetic-wave frequency

From result of Figure 9, it is fined and introduced the relationship among electric impedance, frequency of electromagnetic-wave, and generation of heat energy.

Where, generations of energy are represented eq. (20) ~ (22). W_{CCP} is an energy work of an electromagnetic-wave generator[J/s]. $W_{Z'_{CCP}}$ is an energy work of real part of impedance [J/s]. $W_{Z''_{CCP}}$ is an energy work of imaginary part of impedance [J/s]. $W_{Z'_{CCP}}$ means energy of direct resistance element and this is used to generate a heat energy. On the other hand, $W_{Z''_{CCP}}$ means energy of capacitance element and this is used save a generator's energy. $W_{Z''_{CCP}}$ doesn't change a heat energy and it return to a generator

From the results of Figure 9 and Table 1, it finds that if it wants to increase generation of heat energy, it uses higher frequency. Because if it input higher frequency, it is able to suppress the influence of saving energy $W_{Z''_{CCP}}$.

$$W_{CCP} = \frac{V^2}{|Z_{CCP}|} \tag{20}$$

$$W_{Z'_{CCP}} = \frac{V^2}{|Z'_{CCP}|} \tag{21}$$

$$W_{Z''_{CCP}} = \frac{V^2}{|Z''_{CCP}|} \tag{22}$$

C) Feasibility of heat energy control

Usually, RFA uses frequency of electromagnetic-wave at 470[kHz]. In this paper, we suggested that our system control use of frequency 470±200 [kHz]. From the results of Figure 9, it is supposed that heat energy is able to be controlled approximately ±4% in the frequency range central focus on 470[kHz] at in case of 10.0[V] input. These heat energy control values are almost same between collapse and aerated lung. Especially in case of aerated lung, the effectiveness of electromagnetic-wave frequency control has influence on a value of heat energy. Because lung's internal air volumes increase, electrical impedance increases and a value of heat energy decrease. Thus, it is supposed that our proposal control method has small effectiveness for increase heat energy even if lung include large amount of air.

VI. CONCLUSION AND FUTUREWORK

In this paper, we modeled and analyzed electric impedance frequency characteristic of lung with change of lung' internal air volumes to control ablation energy by control of electromagnetic-wave frequency. The electrical impedance model realized high accurate model. The model represented behavior of lung's electrical impedance which consider about non-linearity of electrical properties. From the numerical calculation results, control of electromagnetic wave frequency has a possibility that ablation energy is able to be controlled ±4% in the frequency range central focus on 470±200 [kHz] at in case of 10.0[V] input.

On Future work, we will develop our proposal robotized RF-ablation support systems, and evaluate the value of actual ablation energy comparison with values of our proposal model. In order to evaluate relation between electrical impedance and heat energy, we will relate lung's internal pressure as lung's internal volumes exactly. Finally, we will develop optimal control method for control of electromagnetic-wave frequency.

REFERENCES

[1] S. N. Goldberg, "Radiofrequency tumor ablation: principles and techniques," European Journal of Ultrasound, vol.13, pp. 129-147, 2001

[2] C. L. Brace (2009) "Radiofrequency and Micriwave Ablation of the Liver, Lung, Kidney, and Bone: What Are the Differences?", Curr Probl Diagn Radiol

[3] T. Hiraki, H. Gobara, H. Mimura, Y. Sano, T. Tsuda, T. Iguchi, H. Fujiwara, R. Kishi, Y. Matsui, S. Kanazawa, "Does tumor type affect local control by radiofrequency ablation in the lungs?," European Journal of Radiology, vol.74, pp. 136-141, 2010

[4] Nozomu Yamazaki, Hiroki Watanabe, XiaoWei Lu, Yosuke Isobe, Yo Kobayashi, Tomoyuki Miyashita, Masakatsu G. Fujie, "Development of a temperature distribution simulator for lung RFA based on air dependence of thermal and electrical properties", Proceeding of 34rd Annual International Conference of the IEEE Engineering in Medicine and Biology Society, pp. 5699-5702, 2012

[5] N. Yamazaki, H. Watanabe, T. Hoshi, Y. Kobayashi, T. Miyashita, M. G. Fujie, Modeling the Internal Pressure Dependence of Thermal Conductivity and in vitro Temperature Measurement for Lung RFA. Proceeding of 33rd Annual International Conference of the IEEE Engineering in Medicine and Biology Society: 5753-5757, 2011

[6] Yosuke Isobe, et. al., "Real-Time Temperature Control System Based on the Finite Element Method for Liver Radiofrequency Ablation: Effect of the Time Interval on Control", Proceeding of 35rd Annual International Conference of the IEEE Engineering in Medicine and Biology Society, pp. 393 - 397, 2013

[7] Nozomu Yamazaki, et. al., "The relation between temperature distribution for lung RFA and electromagnetic wave frequency dependence of electrical conductivity with changing a lung's internal air volumes", Proceeding of 35rd Annual International Conference of the IEEE Engineering in Medicine and Biology Society, pp. 386 - 391, 2013

[8] Zehn-Gang Zhao and Chuan Li, "Application of Cole-Cole plot to study contact resistance of CNTs humidity sensor", ELECTRONICS LETTERS 28th February 2013 Vol. 49 No. 5

[9] Samir Trabelsi, "Frequency and Temperature Dependence of Dielectric Properties of Chicken Meat", Instrumentation and Measurement Technology Conference (I2MTC), 2012 IEEE International, pp. 1515 – 1518, 2012